Elsevier Editorial System(tm) for European Journal of Medicinal Chemistry
Manuscript Draft

Manuscript Number:

Title: Novel biguanide-based derivatives scouted as TAAR1 agonists: synthesis, biological evaluation, ADME prediction and molecular docking studies.

Article Type: Research Paper

Keywords: Trace amine-associated receptors (TAARs); murine and human TAAR1 agonists; phenyl biguanide derivatives; benzyl biguanide derivatives.

Corresponding Author: Dr. Michele Tonelli, PhD

Corresponding Author's Institution: University of Genoa

First Author: Michele Tonelli, PhD

Order of Authors: Michele Tonelli, PhD; Stefano Espinoza, PhD; Raul Gainetdinov, PhD; Elena Cichero, PhD

Abstract: Trace amines (TAs) are endogenous neuromodulators that play a functional role in the synaptic transmission within central nervous system (CNS), targeting trace amine-associated receptors (TAARs). Starting from our previous computational studies on TAAR1 and TAAR5 interactions with the unselective ligand 3-iodothyronamine (T1AM), we rationally designed and synthesized a new series of biguanide-based compounds that were evaluated in functional activity at murine and human TAAR1 and murine TAAR5 receptors. Among them, phenyl (BIG2, BIG4, BIG8 and BIG22) or benzyl (BIG10-BIG16) biguanides were found to be selective murine and human TAAR1 agonists with potencies in nanomolar or low micromolar range, respectively. In particular, compounds BIG2 and BIG12-BIG14 were the most promising and they could be considered valuable lead compounds worthy of further investigations.
In addition to the interest for developing more effective human TAAR1 ligands, the disclosed here potent murine TAAR1 agonists could offer suitable tools for studying the pharmacology of TAAR1 receptor.

Dear Professor Supuran,

on behalf of all co-authors, I am pleased to submit the enclosed manuscript entitled "*Novel biguanide-based derivatives scouted as TAAR1 agonists: synthesis, biological evaluation, ADME prediction and molecular docking studies*" for publication, as an article, on European Journal of Medicinal Chemistry.

Starting from our previous computational studies on TAAR1 and TAAR5 interactions with the unselective ligand 3-iodothyronamine (**T_1AM**), we rationally designed and synthesized a new series of biguanide-based compounds that were evaluated in functional activity at murine and human TAAR1 and murine TAAR5 receptors. The phenyl and benzyl biguanide derivatives, bearing lipophilic substituents, emerged as two interesting subsets and were of particular interest combining the high activity with more accessible synthetic routs. In fact phenyl (**BIG2**, **BIG4**, **BIG8** and **BIG22**) or benzyl (**BIG10**-**BIG16**) biguanides were found to be selective murine and human TAAR1 agonists with potencies in nanomolar or low micromolar range, respectively. Notably, compounds **BIG2** and **BIG12**-**BIG14** were the most promising and they could be considered valuable lead compounds worthy of further investigations.

In addition to the interest for developing more effective human TAAR1 ligands, the disclosed here potent murine TAAR1 agonists could offer suitable tools for studying the pharmacology of TAAR1 receptor.

Thank you very much and kindest regards.

Yours sincerely,

Michele Tonelli

*Corresponding author.

Phone: +39 010 3538867. E-mail: michele.tonelli@unige.it

Graphical abstract

Novel biguanide-based derivatives scouted as TAAR1 agonists: synthesis, biological evaluation, ADME prediction and molecular docking studies.

Michele Tonelli[a,*], Stefano Espinoza[b], Raul R. Gainetdinov[c,d], Elena Cichero[a,*]

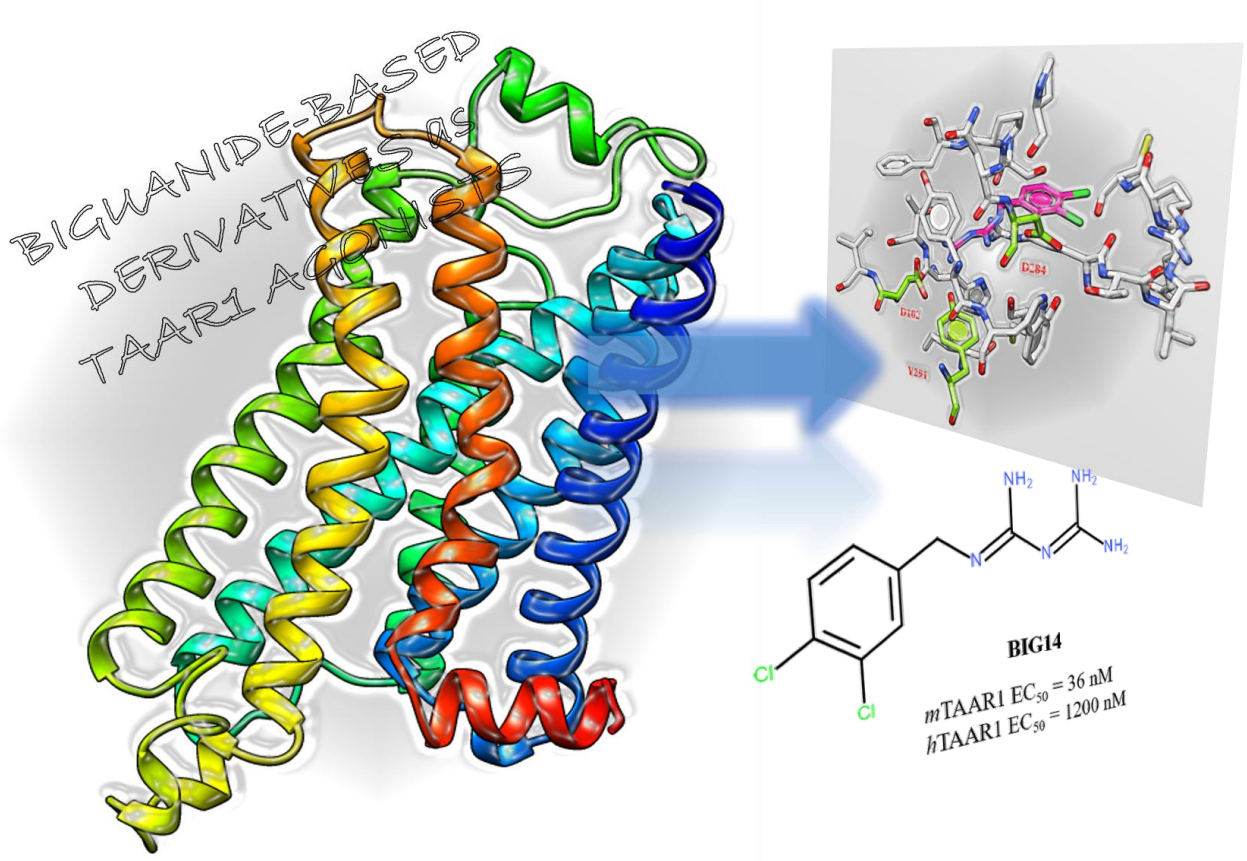

Highlights

- Computationally-driven studies guided for the synthesis of selective TAAR1 agonists
- In this study we prepared linear and cyclic biguanide-based compounds
- Phenyl and benzyl biguanides were found active at murine and human TAAR1 receptors
- Docking studies revealed a bridge role of biguanide moiety in stabilizing H-bonds

Novel biguanide-based derivatives scouted as TAAR1 agonists: synthesis, biological evaluation, ADME prediction and molecular docking studies.

Michele Tonelli[a,*], Stefano Espinoza[b], Raul R. Gainetdinov[c,d], Elena Cichero[a,*]

[a]Department of Pharmacy, University of Genoa, Viale Benedetto XV n. 3, 16132, Genoa, Italy

[b]Department of Neuroscience and Brain Technologies, Istituto Italiano di Tecnologia, Genoa, Italy

[c]Institute of Translational Biomedicine, St. Petersburg State University, 199034, St. Petersburg, Russia

[d]Skolkovo Institute of Science and Technology, Skolkovo, 143025, Moscow Region, Russia

*To whom correspondence should be addressed:

Dr. Michele Tonelli: tel: +390103538867; fax: +390103538399. E-mail: michele.tonelli@unige.it.

Dr. Elena Cichero: tel: +390103538370; fax: + 39 0103538399; E-mail: cichero@unige.it

Abstract

Trace amines (TAs) are endogenous neuromodulators that play a functional role in the synaptic transmission within central nervous system (CNS), targeting trace amine-associated receptors (TAARs). Starting from our previous computational studies on TAAR1 and TAAR5 interactions with the unselective ligand 3-iodothyronamine (**T_1AM**), we rationally designed and synthesized a new series of biguanide-based compounds that were evaluated in functional activity at murine and human TAAR1 and murine TAAR5 receptors. Among them, phenyl (**BIG2**, **BIG4**, **BIG8** and **BIG22**) or benzyl (**BIG10**-**BIG16**) biguanides were found to be selective murine and human TAAR1 agonists with potencies in nanomolar or low micromolar range, respectively. In particular, compounds **BIG2** and **BIG12**-**BIG14** were the most promising and they could be considered valuable lead compounds worthy of further investigations.

In addition to the interest for developing more effective human TAAR1 ligands, the disclosed here potent murine TAAR1 agonists could offer suitable tools for studying the pharmacology of TAAR1 receptor.

Keywords: Trace amine-associated receptors (TAARs), murine and human TAAR1 agonists, phenyl biguanide derivatives, benzyl biguanide derivatives.

1. Introduction

Trace amine-associated receptors (TAARs) belong to the family of G-protein coupled receptors (GPCR), whose first identified member TAAR1 was cloned and deorphanized at the beginning of the twenty-first century by two research groups, working independently [1,2]. Indeed, multiple TAARs genes were identified, which included 9 genes in humans (TAAR1, TAAR2, TAAR5, TAAR6, TAAR8, TAAR9 with TAAR3, TAAR4 and TAAR7 being pseudogenes), 9 in chimpanzees (including 6 pseudogenes), 19 in rats (including 2 pseudogenes), and 16 in mice (including 1 pseudogene). Among them, TAAR1 was the only member initially identified as responsive to a class of biogenic compounds called trace amines (TAs) [3]. TAs, such as tyramines, β-phenylethylamine (β-PEA), octopamines, tryptamine, 3-iodothyronamine (**T_1AM**) and synephrine are found in mammals at low levels

in multiple tissues, both in the periphery and in the brain, but their precise physiological functions have still to be clarified [4].

TAs were described playing a key role as major neurotransmitters in invertebrates, as shown by octopamine that was the most related counterpart of norepinephrine [5,6]. Initially, it was proposed that the main effect determined by TAs was related to sympathomimetic-like actions, and that in any case TAs could behave as neuromodulators of the dopaminergic or adrenergic systems [4]. Accordingly, TAAR1 proved to be expressed in the nigrostriatal and mesolimbic dopaminergic pathways and a number of pharmacological advances pointed out a prominent functional inter-regulation between TAAR1 and dopamine system [7]. As an overall effect, TAAR1 modulate the dopaminergic transmission working as a fine-tuning mechanism [8,9]. Dysfunction of TAs signaling was historically associated to a consistent number of psychiatric diseases believed to be related to alterations in monoaminergic balance [10].

The first receptor types to be investigated was TAAR1, which were expressed in a variety of tissues including brain, stomach, kidney, lung and intestine, but not in the olfactory epithelium (OE). On the contrary, with the exception of TAAR1, all the other TAARs proved to be mainly present in small areas of olfactory sensory neurons (OSNs) in the OE [11].
However, more recent studies revealed biological functions of TAAR2 and TAAR5 receptors beyond olfaction, revealing their presence also at the immune system level and at CNS [12-14]. Indeed, TAAR2 and TAAR5 co-expression with TAAR1 at high levels within human blood leukocytes was recently described, while new evidence pointed out to the presence of TAAR5 in brain regions, such as the ventromedial hypothalamus (VMH) and the amygdala [15].

Despite of these recent findings potentially guiding for innovative therapies in neurons and immune cell system modulation, nowadays the most relevant advances regarding TAARs were based on studies focused on TAAR1 receptor. Growing appreciation of the potential of TAAR1-based pharmacology led to the search for related ligands, mostly due to numerous evidences pointing out that targeting TAAR1 could lead to novel approaches for the treatment of several disorders, such as schizophrenia, depression, attention deficit hyperactivity disorder, Parkinson's disease, addiction and metabolic diseases [16-21].

Up to now, different classes of chemical entities were studied and recognized as TAAR1 ligands, including specific molecules screened and developed as TAAR1 agonists [22] and also known dopaminergic, adrenergic and serotonergic ligands, but at expense of selectivity. On the other hand, only two antagonists were described, including a benzamide-based

derivative, namely RO5212773 (EPPTB) [23], and a phenoxyethylamine-based compound [24]. Conversely, only a few number of TAs were assayed and then identified as TAAR2 or TAAR5 ligands, being **T_1AM** the most investigated.

T_1AM was revealed as a promiscuous TAARs ligand, being able to bind unselectively at least to TAAR1, TAAR2 and TAAR5. In particular, it was found as potent murine TAAR1 agonist (*m*TAAR1 EC_{50} = 189 nM) [25], lowering in potency at the human orthologue receptor (*h*TAAR1 EC_{50} = 1690 nM) [26].

Based on these information, the most critical concerns in the development of effective TAAR1 ligands were firstly selectivity within the TAARs family and further monoamines-directed towards GPCRs, as well as species-specificity variation, as observed around TAs [27].

Recent synthetic efforts were aimed to optimize the efficacy of newly TAAR1 agonists, relying on rational drug design strategies including development of endogenous ligand analogues [25], computationally-driven virtual screenings [24,28] and SOSA approach (Selective Optimization of Side Activities) [29].

In the first case, a series of thyronamine analogues were synthesized leading to compounds whose potency profile toward the *m*TAAR1 falls in the low micromolar range, while by virtual screening approaches Lam and co-workers identified the drug Guanabenz [30] and closely related benzylidene aminoguanidine derivatives [28], exhibiting activity as *m*TAAR1 agonists (Fig. 1).

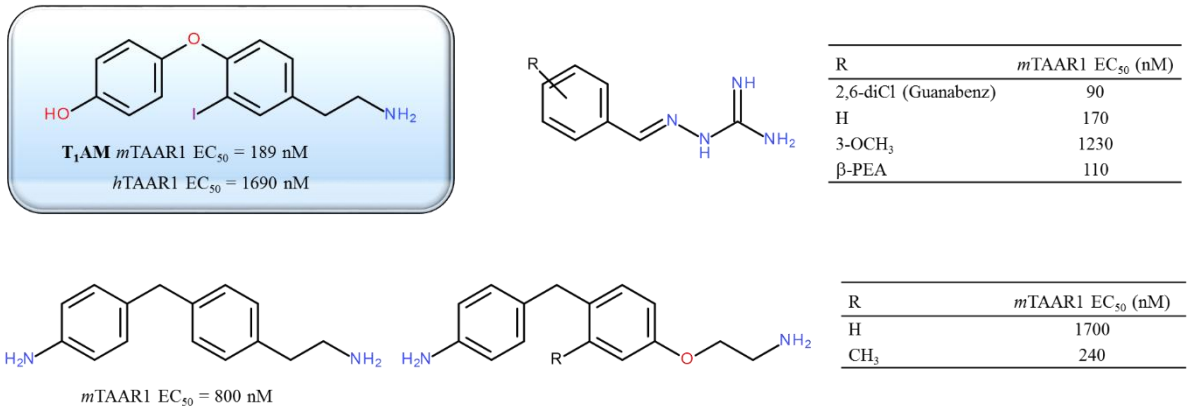

R	*m*TAAR1 EC_{50} (nM)
2,6-diCl (Guanabenz)	90
H	170
3-OCH_3	1230
β-PEA	110

R	*m*TAAR1 EC_{50} (nM)
H	1700
CH_3	240

Fig. 1. Chemical structures and functional data of thyronamine analogues [25] and of Guanabenz and related derivatives [28], studied as *m*TAAR1 ligands. β-PEA was positive control.

More recent SOSA studies performed starting from compounds active towards the adrenoreceptor system, such as the 2-adrenoreceptor partial agonist **S18616**, allowed to derive new series of TAAR1 compounds endowed with improved efficacy also at the *h*TAAR1 receptor. The typical aromatic ring and basic moiety of **S18616** was maintained, modifying the linker region by opening the central six-membered ring. As shown in Fig. 2, following this strategy a number of promising 2-aminooxazolines were developed, acting as *h*TAAR1 agonists or partial agonists.

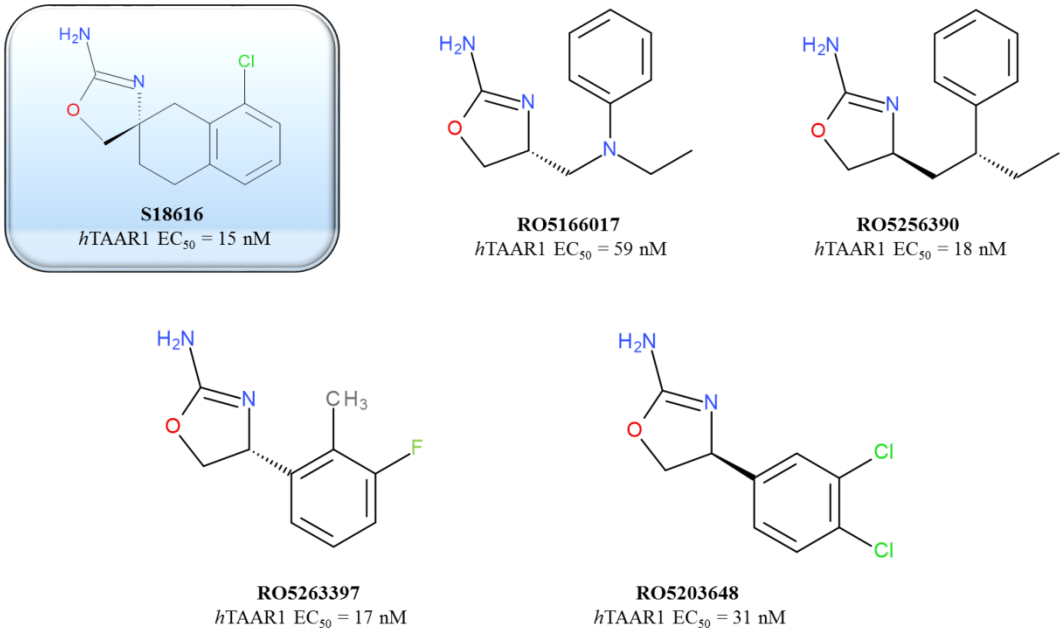

Fig. 2. Chemical structures and functional data of 2-aminooxazolines as *h*TAAR1 ligands [29].

In this context, we started our work exploring TAARs and related ligands applying homology modelling calculations. The computational approach allowed us to build and compare murine and human TAARs models, including TAAR1, TAAR2 and TAAR5 receptors, pointing out any structural feature at their putative binding site that could be involved in ligand recognition. All the models were compared on the basis of docking calculations of the promiscuous ligand 3-iodothyronamine (**T_1AM**), revealing a pattern of key contacts probably responsible for the potency, selectivity profile and species-specificity of TAAR1 ligands [31,32].

In particular, our results promoted the design of small more rigid or planar scaffold bearing proper H-bonding features, rather than the 3-iodothyronamine structure, for the

development of more potent and selective TAAR1 ligands. Based on these results, we proceeded with the synthesis of a new series of compounds exhibiting a biguanide moiety as a rigid basic feature, replacing the flexible ethylamine displayed by **T_1AM**.

The biguanide system is considered an important scaffold endowed with several biological activities: besides the well known properties of currently used therapeutics, as the antidiabetic metformin, the antimalarial proguanil and the antiseptic chlorhexidine, this framework was associated to serotoninergic antagonists [33], antiviral [34-36], anti-H_2 [37,38] and anticancer agents [39,40].

In the present work, we searched for linear (**BIG1**-**BIG23**) and cyclic (**Cyc1**, **Cyc2**) biguanide-based derivatives as novel TAAR chemotypes (Fig. 3), in virtue of their chemical tractability (synthetically accessible and low cost). We have also explored the potential activity of two 2,4-diaminopyrimidines, pyrimethamine (**Cyc3**) and trimethoprim (**Cyc4**), as planar analogues of 4,6-diamino-1,2-dihydrotriazines **Cyc1** and **CyC2** (Fig. 3).

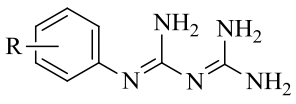

R= H **BIG-1**
R= 2-Cl **BIG-2**
R= 3-Cl **BIG-3**
R= 4-Cl **BIG-4**
R= 3,4-Cl_2 **BIG-5**

R= 3-F **BIG-6**
R= 4-NO_2 **BIG-7**
R= 4-CH_3 **BIG-8**
R= 4-OCH_3 **BIG-9**

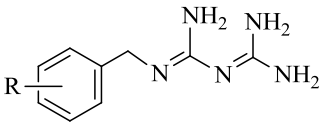

R= H **BIG-10**
R= 2-Cl **BIG-11**
R= 3-Cl **BIG-12**
R= 4-Cl **BIG-13**
R= 3,4-Cl_2 **BIG-14**

R= 3-F **BIG-15**
R= 3-Br **BIG-16**
R= 4-OCH_3 **BIG-17**
R= 3,4-$(OCH_3)_2$ **BIG-18**

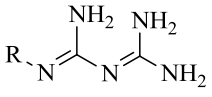

R= cyclopentyl **BIG-19**
R= cycloheptyl **BIG-20**
R= adamant-1-yl **BIG-21**

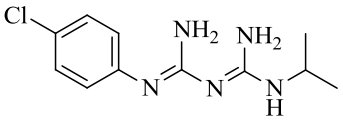

BIG-22 (Proguanil)

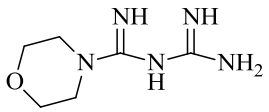

BIG-23 (Moroxydine)

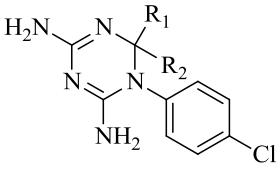

R_1= R_2= CH_3 (Cycloguanil) **Cyc-1**
R_1-R_2= -$(CH_2)_5$- **Cyc-2**

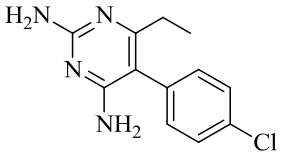

Cyc-3 (Pyrimethamine)

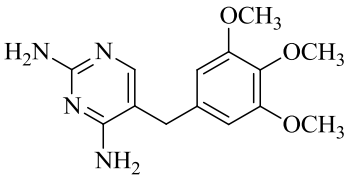

Cyc-4 (Trimethoprim)

Fig. 3. Chemical structures of the investigated TAAR ligands

It is worth noting that the pheyl(benzyl) biguanide system calls back the chemical structure of the previously discussed drug Guanabenz [28] and of the related analogues (Fig. 1).

Thus, twenty-seven compounds have been evaluated in functional activity at murine and human TAAR1 (*m*/*h*TAAR1) and murine TAAR5 (*m*TAAR5) receptors.

These data were accompanied by a thorough *in silico* evaluation of the pharmacokinetic and toxicity properties of the most potent derivatives here disclosed, with the aim at gaining preliminary information concerning their potentially drug-like profile.

These combined studies led to the identification of promising series of molecules to be further optimized as much more effective *h*TAAR1 ligands, but also as *m*TAAR1 agonists, as suitable tools for exploring the TAARs pharmacology.

2. Results and discussion

2.1. Chemistry

Most of the investigated compounds have already been reported in the literature: **BIG2** [41], **BIG3** [42], **BIG5** [43] **BIG6** [44], **BIG7** [45], **BIG8** and **BIG9** [46], **BIG10** [42], **BIG11, BIG12**, **BIG14** and **BIG15** [47].

Compounds **BIG13, BIG16** and **BIG17** were known as free base or nitrate/dipicrate salts [44], while in our synthetic conditions they crystallized directly from the reaction mixture as pure hydrochlorides, thus their experimental properties have been reported herein. **BIG21** [48], moroxydine **BIG23** [44]. Syntheses of compounds **Cyc1** and **Cyc2** were achieved by 3-component syntheses [43].

The novel biguanide compounds **BIG13** and **BIG16**-**BIG20** were synthesized by fusing at 180-200°C for 1 h an equimolar mixture of the proper cycloalkylamine hydrochloride or substituted benzylamine hydrochloride and dicyandiamide (Scheme 1).

In addition to the experimental data, the formation of linear biguanide derivatives was confirmed by pink copper complexes with freshly cuprammonium sulphate solution, in contrast to cyclic biguanides (**Cyc1** and **Cyc2**).

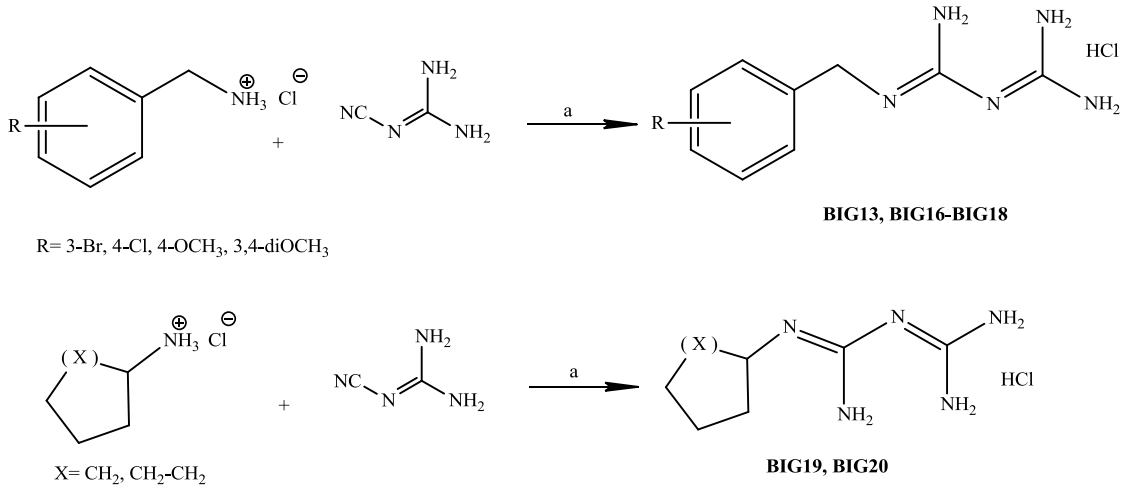

Scheme 1. Reagents and conditions: a) 180-200°C, 1 h.

All new compounds showed excellent analytical and spectroscopic data, in good agreement with their structures (see Experimental Part). The chemical structure of the nonplanar biguanide core has been fully elucidated [49,50] stating, as predominant tautomer, the one without hydrogens at the bridging nitrogens, thus permitting a high degree of conjugation (as for **BIG1**-**BIG22**). In the ^{1}H NMR spectra of the corresponding benzyl biguanide hydrochloride salts, the NH protons give rise to a singlet near δ 9 to 10 and NH_2 groups yield signals in the range δ 7 to 8 [49].

2.2. Molecular docking studies

During the last years, our interest in TAAR pharmacology driven our computational efforts to the development of thorough homology modelling studies around TAAR1 and TAAR5 receptors. The models we derived allowed us to compare the receptors topology and to investigate for ligand potency and selectivity issues [31,32]. Our data suggested that the *m*TAAR1 ligand potency trend was highly related to the presence of a proper basic feature linked to an aromatic core, being the compound engaged in a key salt bridge between a protonated amine group and the highly conserved residue D102, together with a number of π–π stacking and cation-π contacts with the surrounding amino acids [32].

Indeed, for TAAR1 as well as for TAAR5, the interaction with a conserved aspartic acid residue proved to be mandatory, as successively confirmed by Reese for the murine TAAR1 receptor [51].

In particular, according to the results we obtained about **T_1AM**, the compound basic moiety was better stabilized at the *m*TAAR1 rather than at the *h*TAAR1 or *m*/*h*TAAR5, by means of additional H-bonds with surrounding aromatic residues, being these information consistent with the decreasing potency trend of those molecules bearing exclusively a basic feature, moving from the murine to the human species, as described in literature [52].

In addition, the phenolic hydroxyl group of **T_1AM** was in any case H-bonded to the TAAR receptor, while the 3-iodo-phenyl ring showed cation-π contacts with a conserved arginine residue [32]. Notably, the 3-iodo-phenyl core occupied a cavity including hydrophobic and flexible residues (such as leucine and isoleucine) in TAAR5, being conversely in proximity of aromatic and much more rigid amino acids in *m*TAAR1 (such as phenylalanine and tyrosine) or smaller residues (such as valine) in *h*TAAR1.

Thus, the selection of smaller or of much more rigid or planar scaffolds bearing proper H-bonding features emerged to be allowed for the design of more effective TAAR1 ligands, also endowed with an improved selectivity profile with respect to TAAR5.

Based on these results, we deemed interesting to evaluated the possibility to apply a molecular simplification on the chemical structure of **T_1AM**, leading to a new series of compounds lacking of the phenolic portion (which was involved H-bonds within both the TAAR1 and TAAR5 receptors impairing selectivity) and exhibiting a biguanide moiety, instead of the ethylamine chain, as a rigid basic feature.

Docking studies performed at the murine TAAR1 receptor revealed a quite comparable binding mode shared by most of the **BIG** compounds here proposed. In particular, the most promising *para*-substitued phenyl derivatives **BIG4** and **BIG8** were characterized by a net of H-bonds brought by the biguanide moiety and the neighbouring S79, D102, S182 and Y291 residues, moving the phenyl core toward N283 and P280, as displayed by the 3-iodophenyl ring of **T_1AM** (Fig. 4).

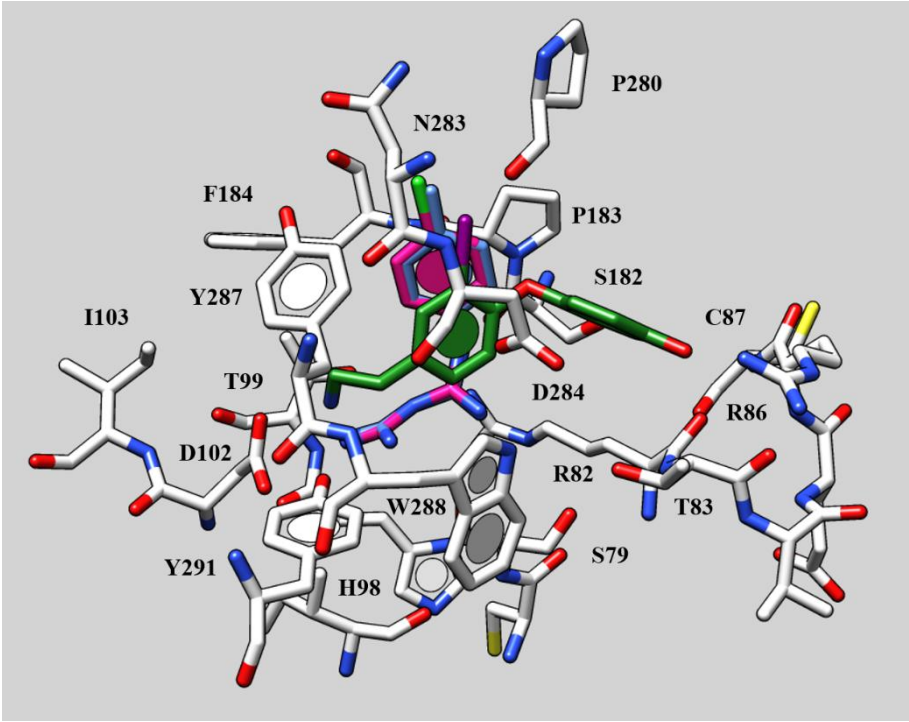

Fig. 4. Docking mode of **T_1AM** (*C* atom; green) and of compounds **BIG4** (*C* atom; deep magenta) and **BIG8** (*C* atom; dark cyan) at the murine TAAR1 binding site. The most important residues are labelled.

It should be noticed that **BIG4** and **BIG8** didn't interact with the binding crevice surrounding the **T_1AM** phenolic substituent, therefore displaying a lower potency profile with respect to the reference compound.

While the aforementioned *para*-substituted derivatives were unable to mimic the **T_1AM** phenolic ring, the *ortho*-substitued **BIG2** adequately moved the chlorine substituent toward the aforementioned region, achieving a better efficacy with respect to the related analogues (Fig. 5).

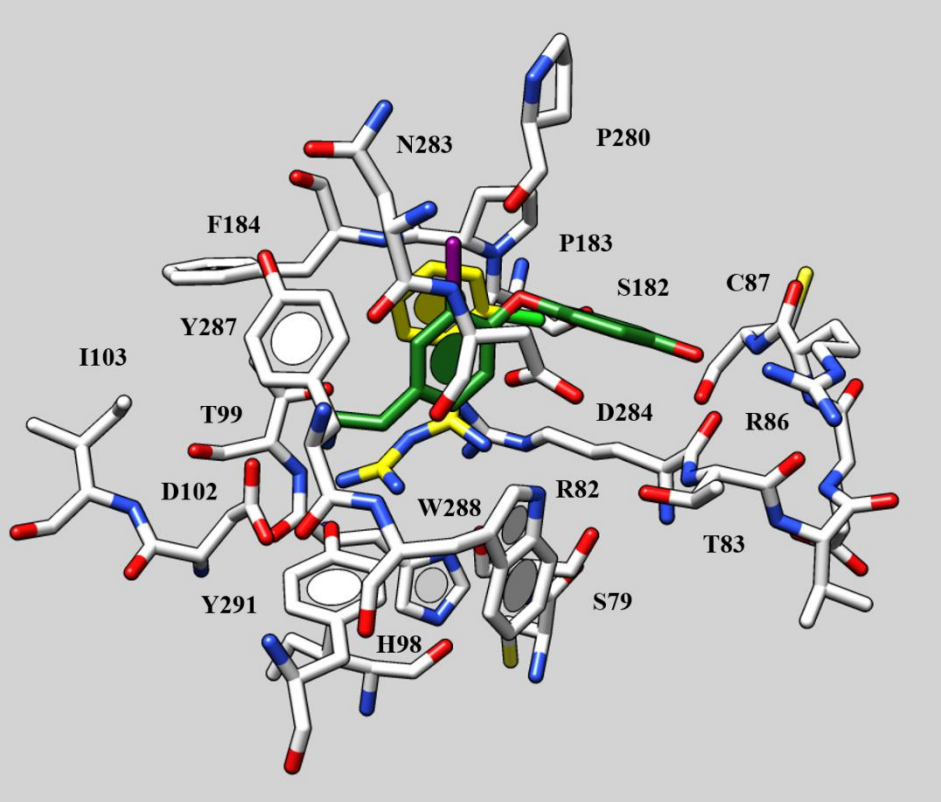

Fig. 5. Docking mode of **T_1AM** (*C* atom; green) and of compound **BIG2** (*C* atom; yellow) at the murine TAAR1 binding site. The most important residues are labelled.

The *orto*- or *para*-substituted benzyl derivatives **BIG11** and **BIG13** arranged the biguanide moiety and the aromatic ring following a highly comparable positioning to that of the phenyl analogue **BIG2**, detecting the same pattern of H-bonds and therefore displaying a similar potency profile (Fig. 1S). Even in these cases, the protein region delimited by T83, R86, C87 and D284 interacting with **T_1AM** was unoccupied by the newly synthesized compounds.

Notably, the *meta*- substitution and also the *meta*- and *para*- di-substitution resulted to be particularly effective for the *m*TAAR1 activity, allowing the benzyl ring to lay within the

receptor binding site in a much more similar way if compared with **T_1AM**. Indeed, the 3-chlorobenzyl-based **BIG12** and the 3,4-dichlorobenzyl analogue **BIG14** appeared to quite overlap the docking mode observed for **T_1AM** through their aromatic ring (Fig. 2S and Fig. 6). In addition, this kind of positioning allowed the biguanide moiety to be engaged in multiple H-bonds contacts with D102 and also to behave as a bridge interacting with D284, leading to a highly stabilized protein-ligand complex, as we discussed in our previous works.

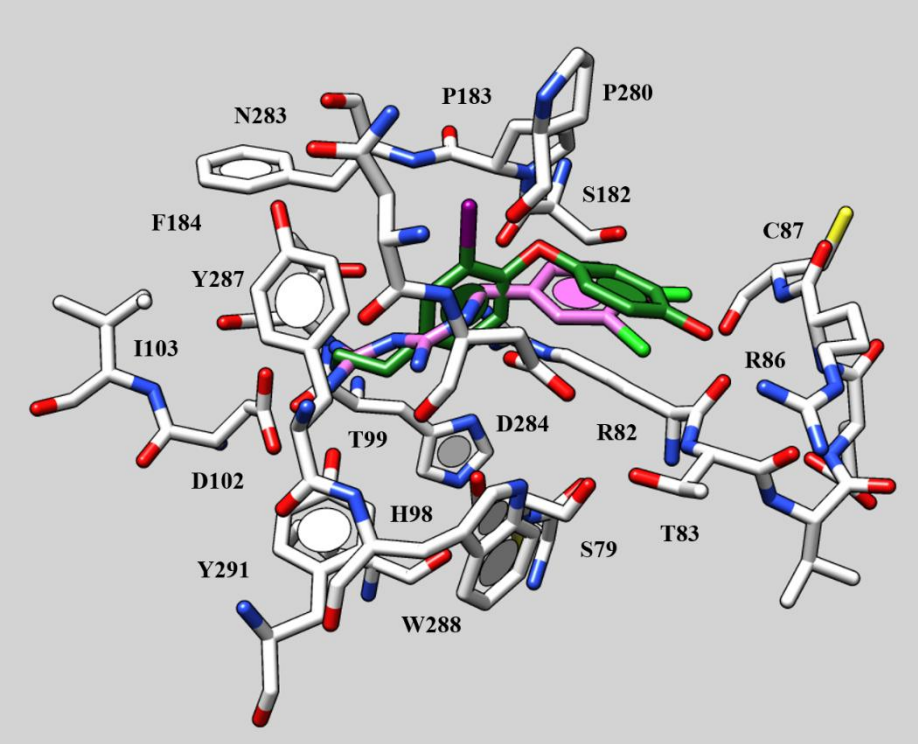

Fig. 6. Docking mode of **T_1AM** (*C* atom; green) and of compound **BIG14** (*C* atom; pink) at the murine TAAR1 binding site. The most important residues are labelled.

Notably, these results were in accordance with the biological data described in the following section, giving an interesting explanation of the improved TAAR1 agonist activity of **BIG12** and **BIG14** if compared with **T_1AM**.

Molecular docking studies within the human TAAR1 receptor were conducted using **S18616** [29] as reference compound, being characterized by a high potency toward the biological target (*h*TAAR1 EC_{50}= 15 nM) and also by a rigid spiro-anellated structure that allow to limit its possible conformational variability within the receptor binding site and therefore to derive much more reliable information.

The primary amine group of the ligand was engaged in H-bonds with the key residue D103 and Y294 while the aromatic portion was placed in a receptor cavity delimited by R83, S183, N286, D287 (Fig. 3S). In particular, **S18616** was stabilized within the *h*TAAR1 binding site by cation-π contacts with R83 and also due to a H-bond acceptor-like behaviour played by the chlorine atom with respect to the N286 side-chain.

Regarding the newly synthesized biguanide-based compounds, the driving force moving the ligand positioning within the receptor cavity was highly related to the possibility to contact N286, as we previously discussed for **S18616**. Indeed, the phenyl derivatives **BIG2**, **BIG4** and **BIG8** placed the aromatic core in proximity of that of the reference compound, being only the *orto*-substituted **BIG2** able to weakly mimic the **S18616** chlorine (Fig. 7).

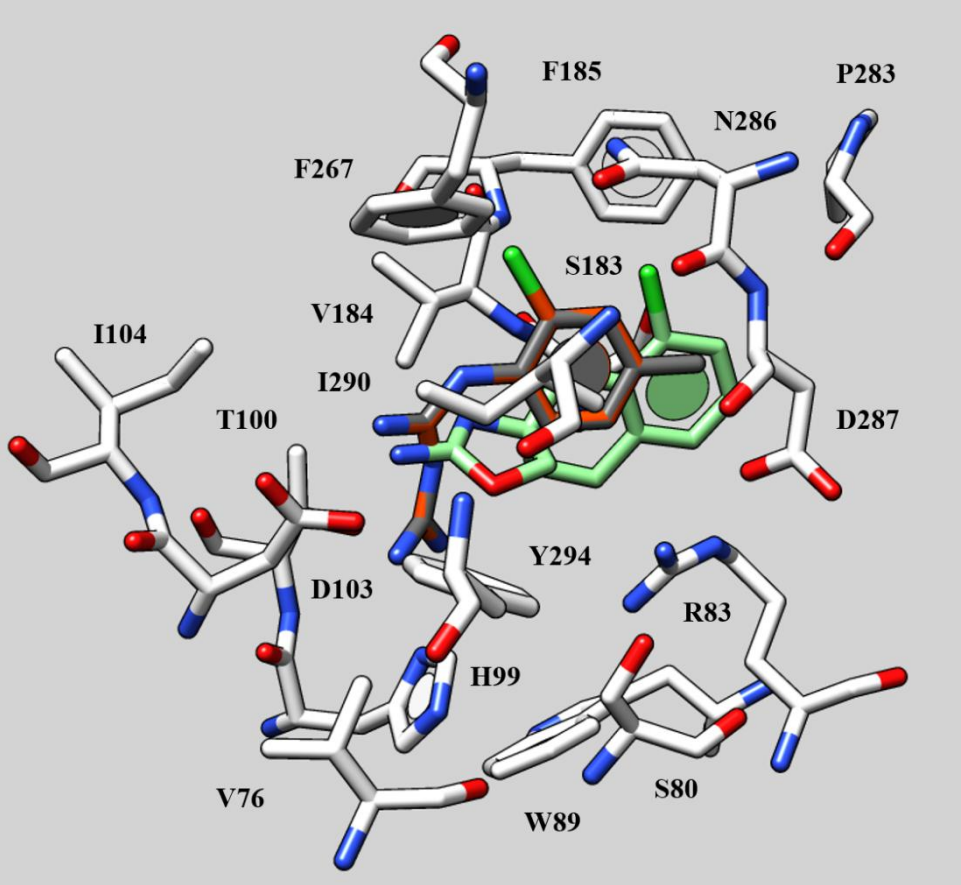

Fig. 7. Docking mode of **S18616** (*C* atom; light green) and of compounds **BIG2** (*C* atom; orange) and **BIG4** (*C* atom; dark grey) at the human TAAR1 binding site. The most important residues are labelled.

Accordingly, **BIG2** was the only phenyl derivative endowed with an acceptable *h*TAAR1 agonist activity, being on the contrary the related 4-chlorophenyl (**BIG4**) and 4-tolyl (**BIG8**) analogues inactive.

Concerning the biguanide moiety, it appeared to be H-bonded to H99, D103 and Y294, being a good bioisostere of the **S18616** aminooxazoline ring.

The introduction of a benzyl moiety instead of the phenyl ring led to much more promising *h*TAAR1 ligands (**BIG11-16**), whose putative binding mode included H-bonds with S80, D103 and Y294, similarly to the corresponding pattern of contacts shown by the **S18616** oxazoline cycle (Fig. 8). The overall arrangement of the benzyl group allowed moving the aromatic ring near I290, F185, F267, detecting Van der Waals and π–π stacking interactions. Among these derivatives, the *para*-substitution with an electron-rich atom improved the ligand potency probably reinforcing any possible (weak) polar contact with N286. On the other hand, all the compounds here proposed partially covered the pattern of interactions detected by the bulky spiro-anellated core of **S18616**. Consequently, they displayed in any case moderately weak or poor bonds with the receptor crevice including N286, exhibiting lower potency values than the reference compound. Nevertheless, especially this series of derivatives could be further optimized as *h*TAAR1 ligands thanks to a proper selection of substituents to be placed at the benzyl *para* position or modifying the benzyl core with a bulkier aromatic/heteroaromatic systems.

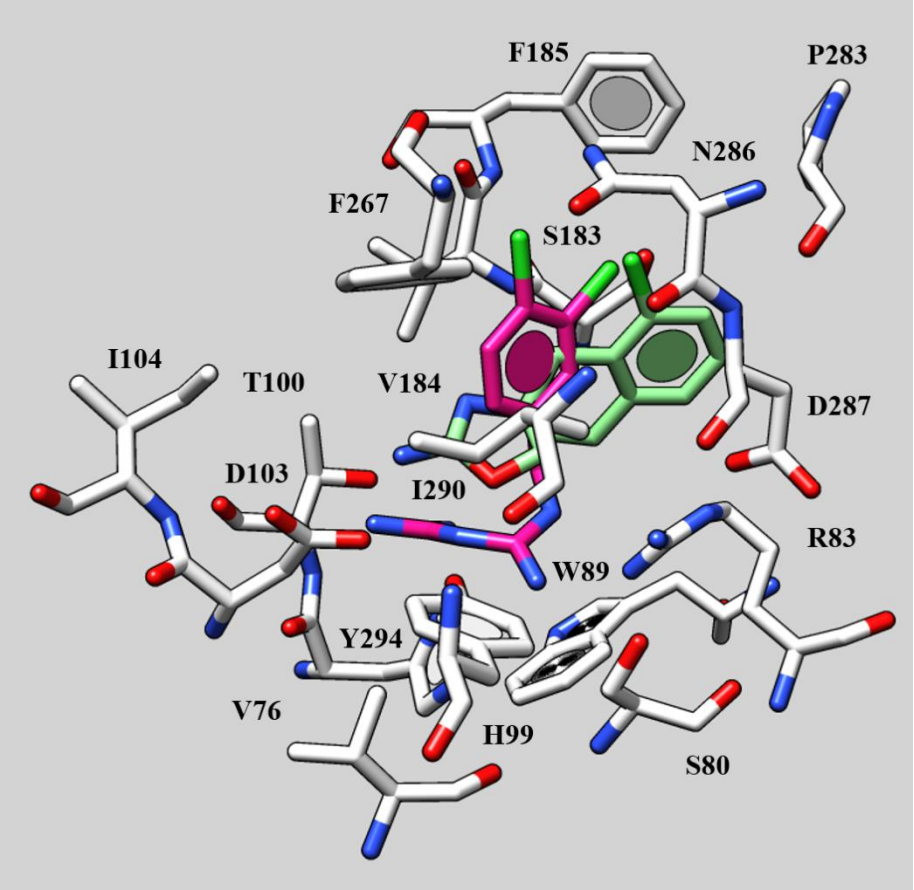

Fig. 8. Docking mode of **S18616** (*C* atom; light green) and of compound **BIG14** (*C* atom; deep magenta) at the human TAAR1 binding site. The most important residues are labelled.

2.3. ADME in silico evaluation

Nowadays, the computational prediction of descriptors representing absorption, distribution, metabolism, excretion and toxicity properties (ADMET) are considered useful *in silico* tools, accelerating the lead compound discovery process [53].

Thus, for the active **BIG** compounds we evaluated a series of ADMET properties, also taking into account the related parameters calculated for two potent *h*TAAR1 ligands described in literature, RO5256390 and RO5263397, whose favourable pharmacokinetic profile was experimentally determined [29]. Briefly, RO5256390 and RO5263397 were characterized by an acceptable human hepatocyte clearance and inhibitory activity of the cytochrome isoforms, displaying an *in vitro* safety profile performed by (negative) AMES/MNT test and *h*ERG IC_{50} evaluation. Based on these data the two compounds were retained as development candidates as partial TAAR1 agonists. Notably, in our compound series the plasmonicidal drug proguanil **(BIG22)** was also included: as known, it is slowly but adequately absorbed *per os*, it is partially metabolized by CYP2C subfamily to the active

metabolite cycloguanil and is excreted in the urine. It is considered well-tolerated and safe [54].

In this work, for the aforementioned compounds, the logarithmic ratio of the octanol-water partitioning coefficient (cLogP), extent of blood-brain barrier permeation (LogBB), rate of passive diffusion-permeability (LogPS), human intestinal absorption (HIA), volume of distribution (Vd), the role played by plasmatic protein binding (%PPB) and by the ligand affinity toward the human serum albumin ($LogK_a^{HSA}$) were taken into account (Table 1).

The putative metabolism and toxicity profiles of any compound was determined on the basis of a number of descriptors such as the compound potential behaviour as P-glycoprotein inhibitor or substrate, the ability to interact with the endocrine system and to act as cytochrome P450 3A4 inhibitor or substrate, the median lethal dose (LD_{50}) related to oral administration (see Table 2).

Table 1. Calculated ADMET descriptors related to absorption and distribution properties.

Comp.	cLogP	LogBB[a]	LogPS[b]	HIA (%)[c]	Vd (l/kg)[d]	%PPB	$LogKa^{HSA}$	%F (oral)
BIG2	1.36	0.14	-3.5	48	3.2	30	3.14	28.8
BIG4	1.22	0.08	-3.3	53	3.5	42	2.99	32.3
BIG8	0.94	0.08	-3.7	43	3.5	27	2.55	25.1
BIG10	-0.17	-0.02	-4.6	39	3.3	12	2.41	22.2
BIG11	0.88	-0.03	-4.2	35	3.5	27	2.74	19.5
BIG12	0.88	-0.03	-4.2	35	3.5	27	2.74	19.5
BIG13	0.88	-0.03	-4.2	35	3.7	27	2.74	19.5
BIG14	0.84	-0.11	-4.2	31	3.9	40	3.14	16.9
BIG15	-0.16	-0.01	-4.6	38	3.1	11	2.42	21.8
BIG16	0.80	-0.02	-4.3	33	3.7	23	2.60	18.3
BIG22	2.32	0.38	-3.1	75	5.4	52	3.19	51.0
RO5256390	2.62	0.46	-2.0	100	4.0	63	3.19	99.3
RO5263397	1.92	0.35	-2.0	100	2.4	28	3.12	99.0

[a]Extent of brain penetration based on ratio of total drug concentrations in tissue and plasma at steady-state conditions; [b]Rate of brain penetration. PS represents Permeability-Surface area product and is derived from the kinetic equation of capillary transport; [c]HIA represents the human intestinal absorption, expressed as percentage of the molecule able to pass through the intestinal membrane; [d]prediction of Volume of Distribution (Vd) of the compound in the body.

As shown in Table 1, all the compounds with the exception of **BIG10** and **BIG15** were characterized by an adequate lipophilicity, being the calculated cLogP below 5 (Lipinski rules) and that of **BIG2** comparable with the one of RO5263397 . Among the most active compounds, **BIG2** was endowed with the ability to be partially adsorbed at the human

intestinal membrane (HIA = 48%). Notably, all the derivatives shown poor blood-brain barrier (BBB) permeation for passive diffusion, showing LogBB and/or LogPS values falling sometimes out of the recommended ranges (0<LogBB<1.5; -3<LogPS<-1). Nevertheless, all of them were predicted to penetrate the BBB by means of active transport carrier.

The calculated volume of distribution values and also the potential binding to the plasmatic proteins fall in the allowed ranges and in any case within those displayed by RO5256390 and RO5263397. In particular **BIG2** and **BIG14** were characterized by the most similar Vd and %PPB values.

According to an overall analysis of the descriptors listed in Table 2, none of the compounds here proposed should be substrate of the P-glycoprotein, or be involved in genotoxicity events such as binding with the endocrine system. Indeed, all the derivatives were characterized by acceptable LogRBA values, being lower than -3 within high reliability indices.

Furthermore, none of them proved to inhibit the cytochrome P450 3A4, being on the contrary substrate for the enzyme at lower values than that displayed by RO5256390 and RO5263397.

Notably, all of them exhibited a favourable safety profile, being the estimated LD_{50} in the range of 640-1400 mg/kg for mouse after oral administration, being in any case higher than those calculated for the two development candidate RO5256390 and RO5263397.

Table 2. Calculated ADMET descriptors related to metabolism, excretion and toxicity properties.

Comp.	P-glycoprotein		Endocrine System Disruption[a]		CYP3A4		LD_{50}[b] (mg/kg) (R.I.≥ 0.60)
	Inhib.	Substrate (R.I.≥ 0.40)	LogRBA> -3 (R.I.≥ 0.50)	LogRBA> 0 (R.I.≥ 0.80)	Inhib.	Substrate (R.I.≥ 0.50)	
BIG2	not	not	0.12	0.00	not	0.05	370
BIG4	not	not	0.06	0.00	not	0.04	400
BIG8	not	not	0.06	0.00	not	0.05	990
BIG10	not	not	0.01	0.00	not	0.05	710
BIG11	not	not	0.03	0.00	not	0.11	690
BIG12	not	not	0.03	0.00	not	0.11	690
BIG13	not	not	0.03	0.00	not	0.10	690
BIG14	not	not	0.05	0.00	not	0.10	600
BIG15	not	not	0.01	0.00	not	0.07	580
BIG16	not	not	0.04	0.00	not	0.10	680
BIG22	not	not	0.06	0.01	not	0.21	190
RO5256390	not	not	0.05	0.01	not	0.32	160
RO5263397	not	not	0.03	0.01	not	0.33	47

[a]RBA represents the relative binding affinity with respect to that of estradiol. Compounds showing LogRBA> 0 are classified as strong estrogen binders, while those showing LogRBA< -3 are considered as non-binders. [b]Acute toxicity (LD_{50}) for mouse after oral administration (RI: reliability index. Borderline-allowed values for reliabity parameter are ≥0.3, the most predictive fall in the range 0.50-1.0); [c]MRDD represents the maximum recommended daily dose.

3. Biological evaluation

3.1. Structure-activity relationships of biguanide derivatives on m/hTAAR1.

Twenty-two linear biguanides (**BIG1-BIG22**), two 4,6-diamino-1,2-dihydrotriazines (**Cyc1-Cyc2**) and two 2,4-diaminopyrimidines (**Cyc3-Cyc4**) considered in this work were evaluated for functional activity at *m*/*h*TAAR1 and *m*TAAR5 receptors (Table 3). Unfortunately, the absence of a potent compound stimulating the human form prevents setting up a related pharmacological protocol about *h*TAAR5.

The activity of the compounds was measured using HEK-293 cells transfected with *m*/*h*TAAR1 or *m*TAAR5, or empty vector as control, and a cAMP BRET biosensor. β-PEA was used as positive control for agonism. In the initial screening phase, all the compounds were tested at 10 μM either for agonistic or antagonistic activity. Then for the compounds that were active, a dose-response experiment was performed using concentrations ranging from 10 nM to 100 μM in order to calculate their corresponding EC_{50} values. The Emax value for the functional activity data at TAARs describes the degree of functional activity

compared to 100% for the natural ligand and full agonist β-PEA. All the compounds displayed an Emax>85% at *m*/*h*TAAR1, thus they were regarded as full agonist.

The species-specificity ratio (SSR) of *m*TAAR1 versus *h*TAAR1 is determined by dividing the *h*TAAR1 EC_{50} value by the *m*TAAR1 EC_{50} value (Table 3).

Table 3. Functional activity at *m*/*h*TAAR1 and *m*TAAR5 receptors for compounds **BIG1-BIG23** and **Cyc1-Cyc4**.[a,b]

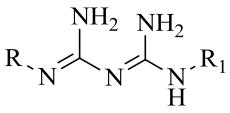

Compds	R	R_1	EC_{50} (nM)		Species-Specificity Ratio
			*m*TAAR1	*h*TAAR1	
BIG2	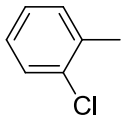	H	410	1000	2.44
BIG4	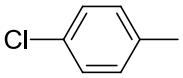	H	2100	>10000	>4.76
BIG8	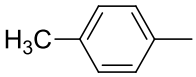	H	1700	>10000	>5.88
BIG10	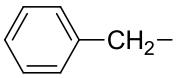	H	780	>10000	>12.82
BIG11	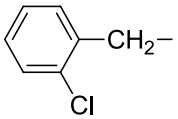	H	410	3000	7.31
BIG12	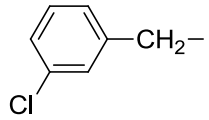	H	97	7000	72.16
BIG13	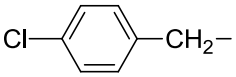	H	780	1800	2.31
BIG14	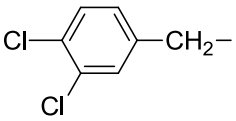	H	36	1200	33.33
BIG15	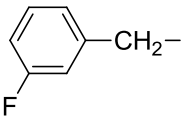	H	540	1600	2.96
BIG16	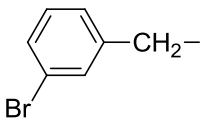	H	1800	4900	2.72
BIG22	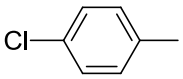	*i*Pr	5400	>10000	>1.85

[a] Only the compounds active as *m*/*h*TAAR1 ligands are listed. [b]All the compounds were shown inactive as *m*TAAR5 ligands up to the highest concentration tested (EC_{50}> 10 μM).

The active compounds were found selective only for TAAR1 subtype, leaving unaffected *m*TAAR5. Activity is displayed only by phenyl (**BIG2**, **BIG4**, **BIG8** and **BIG22**) or benzyl (**BIG10**-**BIG16**) biguanides, while dihydrotriazine and pyrimidine scaffolds were responsible for lacking (losing) of any activities against the investigated targets. Eleven out of twenty-seven compounds exhibited *m*TAAR1 agonistic behavior with EC_{50} values in the range 36-5400 nM, while 64% of them was also able to target *h*TAAR1 with low micromolar potency.

All the active compounds on both *m*/*h*TAAR1 subtypes bore lipophilic substituents (Cl, F, Br, CH_3) on the aromatic ring, with the electron-withdrawing chlorine atom as the best substitution, instead polar groups (OCH_3, NO_2) resulted detrimental (**BIG7**, **BIG9**, **BIG17** and **BIG18**).

In particular within the phenyl biguanides subset, the most potent *m*TAAR1 agonist was the 1-(*ortho*-chlorophenyl)biguanide (**BIG2**) with an EC_{50}= 410 nM, while the corresponding *para*-Cl (**BIG4**) and *meta*-Cl isomers (**BIG3**) showed a 5-fold decrease or even loss of activity, respectively. In the case of the antimalarial drug proguanil (**BIG22**), the simultaneous presence of 1-(4-chlorophenyl) ring and the bulky 5-*iso*propyl group on the biguanide moiety is responsible for a reduction of activity that reached the highest EC_{50} value equal to 5400 nM. Besides halogens, also the apolar and electron-donor *para*-CH_3 substituent was permitted, but providing a lower efficacy (**BIG8**)**.**

In the benzyl biguanides subset, the mono-Cl substitution in *meta*-position increased the activity at *m*TAAR1 (**BIG12**, EC_{50}= 97 nM), whereas *ortho*- and *para*-substitutions were less favorable with a 4-fold (**BIG11**) or 8-fold (**BIG13**) decreases of the potency. Having assumed the *meta*-Cl substituent as the best suited in this subset, firstly the isosteric replacement of chlorine with fluorine or bromine atoms was also explored, however obtaining less effective agonists (**BIG15**, **BIG16**) which displayed EC_{50} values of 540 and 1800 nM, respectively. Indeed, the combination of *meta*- and *para*-substitutions with two chlorine atoms led to the most potent tested derivative (**BIG14**), exhibiting an EC_{50}= 36 nM.

Concerning the activity at *h*TAAR1, SARs moved with a slightly different trend compared to *m*TAAR1: first compound **BIG2** was found the only active representative of phenyl biguanide system and the most potent with an EC_{50}= 1000 nM, whilst the 3,4-dichlorobenzyl derivative **BIG14** ranked second for efficacy (EC_{50}= 1200 nM). Regarding the effect of mono-substitution on the benzyl moiety, the *para*-Cl group was more tolerated than *ortho*-Cl and *meta*-Cl, since compound **BIG13** (EC_{50}= 1800 nM) was 1.7-fold and 3.9-fold more active than **BIG11** and **BIG12**, respectively. Unlike the aforementioned excellent activity at

*m*TAAR1 of **BIG12**, for *h*TAAR1 the *meta*-Cl substitution was less favorable than *meta*-Br (**BIG16**) and, even more, than *meta*-F (**BIG15**) ones.

In Table 3 the species-specificity ratio (SSR) values are also listed, in order to highlight species-specific differences influenced by variation of the chemical space on the biguanide skeleton. All the compounds shared a better agonist behavior versus *m*TAAR1 with respect to *h*TAAR1 and, in particular, compounds **BIG12** and **BIG14** displayed the highest SSR values equal to 72.16 and 33.33, respectively.

Compound **BIG13**, although 21.6-fold and 1.5-fold less active at *m*TAAR1 and *h*TAAR1, respectively, than **BIG14**, possessed the lowest specificity ratio (SSR= 2.31), thus suggesting that the mono-substitution in *para*-position with a lipophilic group on the benzyl biguanide scaffold was the well-suited, capable of enhancing activity versus *h*TAAR1.

Finally, concerning the phenyl biguanide subset, only the *ortho*-substitution on the aromatic ring with a chlorine atom was responsible for a low SSR value comparable to that of **BIG14**, as shown by the most active *h*TAAR1 agonist **BIG2** (SSR=2.44)**.**

4. Conclusions

Herein we described the discovery of potent and selective *m*/*h*TAAR1 agonists, characterized by a biguanide moiety. Notably, the phenyl and benzyl biguanide derivatives, bearing lipophilic substituents, emerged as two interesting subsets and were of particular interest combining the high activity with more accessible synthetic routs. Thus, compounds **BIG2** and **BIG12-BIG14** were the most promising and they could be considered valuable lead compounds worthy of further investigations. In view of a future chemical optimization, the analysis of the *in vitro* TAAR1 activity data reported in this work suggested the following observations: a) the importance of a rigid scaffold, such as the biguanide one, to obtain an improved selectivity profile versus TAAR1 with respect to TAAR5; b) a benzyl biguanide scaffold substituted in *para*-position with lipophilic groups, or replaced by bulkier aromatic or heteroaromatic rings for an improved species-specificity versus *h*TAAR1; c) a planar phenyl biguanide system substituted in *ortho*-position with apolar groups, for the design of potent *h*TAAR1 ligands. In addition to the interest for developing more effective *h*TAAR1 ligands, nevertheless the here disclosed potent *m*TAAR1 agonists (**BIG14** and **BIG12**) could offer suitable tools for studying the pharmacology of TAAR1 receptor.

5. Experimental section

5.1. Chemistry

5.1.1. General methods

Chemicals, solvents and commercially available compounds [1-phenylbiguanide hydrochloride (**BIG1**), 1-(4-chlorophenyl)biguanide hydrochloride (**BIG4**), proguanil (**BIG22**), pyrimethamine (**Cyc3**) and trimethoprim (**Cyc4**)] were purchased from Sigma-Aldrich (Milan, Italy). Column chromatography (CC): neutral alumina (Al_2O_3), activity 1 (Merck) or silica gel. Mps: Büchi apparatus, uncorrected. ^{1}H NMR spectra and ^{13}C NMR spectra: Varian Gemini-200 spectrometer; $CDCl_3$ or DMSO-*d6*; d in ppm rel. to Me4Si as internal standard. J in Hz. Elemental analyses were performed on a Carlo Erba EA-1110 CHNS-O instrument in the Microanalysis Laboratory of the Department of Pharmacy of Genoa University. The NMR spectra of compounds **BIG13** and **BIG16**-**BIG20** are shown in the Supplementary data. Results of elemental analyses and NMR spectra indicated that the purity of all compounds was ≥95%.

5.1.2. General method for the synthesis of biguanide derivatives

A mixture of proper cycloalkyl- or benzylamine hydrochloride (2.6 mmol) and cyanoguanidine (2.6 mmol) was heated at 180-200°C. The molten mass was maintained at the same temperature for 1 h. After cooling the hard solid residue was dissolved in MeOH and the solution concentrated under vacuum, affording the title monohydrochloride (cpds. **BIG19**, **BIG20**). In the case of benzylbiguanide derivatives (**BIG13** and **BIG16**-**BIG18**) the monohydrochloride salts were high hygroscopic, thus the residues were directly converted into the more stable dihydrochloride salts with 1N ethanolic solution of HCl.

*5.1.3. 1-(4'-Chlorobenzyl)biguanide dihydrochloride (**BIG13**)*

Yield: 69%. Mp 215-218°C (dec.). ^{1}H NMR (200 MHz, $CDCl_3$): 4.26-4.63 (m, 2 H, N*C*H_2-Ar), 7.08-7.80 (m, 8H, 4 ArH and 2NH_2 that exchange with D_2O), 8.57 (br. s, NH_2, exchange with D_2O), 9.28 (br. s, $^+$NH, exchange with D_2O), 9.91 (br. s, $^+$NH, exchange with D_2O). ^{13}C NMR (50 MHz, $CDCl_3$): 157.99, 136.09, 131.59, 130.61, 129.54, 128.69, 128.06, 42.71. Anal. Calcd for $C_9H_{12}ClN_5$+ 2HCl+ 0.2H_2O: C, 35.77; H, 4.80; N, 23.17. Found: C, 35.84; H, 4.79; N, 23.22.

*5.1.4. 1-(3'-Bromobenzyl)biguanide dihydrochloride (**BIG16**)*

Yield: 76%. Mp 221-224°C (dec.). ^{1}H NMR (200 MHz, $CDCl_3$): 4.26-4.63 (m, 2 H, N*C*H_2-Ar), 7.00-7.75 (m, 8H, 4 ArH and 2NH_2 that exchange with D_2O), 8.54 (br. s, NH_2, exchange with D_2O), 9.28 (br. s, $^+$NH, exchange with D_2O), 9.89 (br. s, $^+$NH, exchange with

D_2O). ^{13}C NMR (50 MHz, $CDCl_3$): 157.78, 140.05, 130.24, 129.50, 126.89, 126.00, 121.33, 42.48. Anal. Calcd for $C_9H_{12}BrN_5$+ 2HCl+ $0.2H_2O$: C, 31.18; H, 4.19; N, 20.20. Found: C, 31.42; H, 4.35; N, 20.14.

*5.1.5. 1-(4'-Methoxybenzyl)biguanide dihydrochloride (**BIG17**)*

Yield: 84%. Mp 200-204°C (dec.). ^1H NMR (200 MHz, $CDCl_3$): 3.74 (s, 3H, OCH_3), 4.23-4.50 (m, 2 H, N*CH*$_2$-Ar), 6.92 (d, *J* = 8.4, 2H, ArH), 7.10-7.60 (m, 6H, 2ArH and $2NH_2$ that exchange with D_2O), 8.50 (br. s, NH_2, exchange with D_2O), 9.20 (br. s, $^+$NH, exchanges with D_2O), 9.87 (br. s, $^+$NH, exchange with D_2O). ^{13}C NMR (50 MHz, $CDCl_3$): 158.21, 156.68, 129.15, 128.70, 128.33, 113.46, 54.74, 42.98. Anal. Calcd for $C_{10}H_{15}N_5O$+ 2HCl+ $0.2H_2O$: C, 40.33; H, 5.89; N, 23.52. Found: C, 40.53; H, 5.85; N, 23.57.

*5.1.6. 1-(3,4-Dimethoxybenzyl)biguanide dihydrochloride (**BIG18**)*

Yield: 80%. Mp 181-184°C (dec^1H NMR (200 MHz, $CDCl_3$): 3.73 (s, 6H, $2OCH_3$), 4.22-4.54 (m, 2 H, N*CH*$_2$-Ar), 6.73-7.65 (m, 7H, 3 ArH and $2NH_2$ that exchange with D_2O), 8.60 (br. s, NH_2, exchange with D_2O), 9.30 (br. s, NH^+, exchange with D_2O), 9.88 (br. s, NH^+, exchanges with D_2O). ^{13}C NMR (50 MHz, $CDCl_3$): 158.08, 156.80, 148.31, 148.07, 129.11, 120.15, 119.16, 111.88, 55.19, 43.40. Anal. Calcd for $C_{11}H_{17}N_5O_2$+ 2HCl+ $0.25H_2O$: C, 40.19; H, 5.98; N, 21.31. Found: C, 40.27; H, 6.00; N, 21.44.

*5.1.7. 1-Cyclopentylbiguanide hydrochloride (**BIG19**)*

Yield: 78%. Mp 240-241°C. ^1H NMR (200 MHz, $CDCl_3$): 1.20-2.00 (m, 8 H, $4CH_2$ cyclopentane), 3.89 (pseudo s, 1 H, CH, cyclopentane), 6.95 (br s, 6 H, $3NH_2$, exchange with D_2O), 7.74 (br s, 1 H, $^+$NH, exchanges with D_2O). ^{13}C NMR (50 MHz, $CDCl_3$): 159.96, 157.79, 51.90, 31.99, 22.78. Anal. Calcd for $C_7H_{15}N_5$ +HCl: C, 40.87; H, 7.84; N, 34.05. Found: C, 40.88; H, 7.89; N, 33.88.

*5.1.8. 1-Cycloheptylbiguanide hydrochloride (**BIG20**)*

Yield: 69%. Mp 198-201°C. ^1H NMR (200 MHz, $CDCl_3$): 1.04-1.90 (m, 12H, $6CH_2$ cycloheptane), 3.64 (pseudo s, 1 H, CH, cycloheptane), 6.56-7.20 (m, 6 H, $3NH_2$, exchange with D_2O), 7.55 (br s, 1 H, $^+$NH, exchanges with D_2O).). ^{13}C NMR (50 MHz, $CDCl_3$): 162.54, 159.46, 157.17, 50.98, 33.94, 27.32, 22.92. Anal. Calcd for $C_9H_{19}N_5$ + HCl+ $0.5H_2O$: C, 44.53; H, 8.72; N, 28.85. Found: C, 44.36; H, 8.75; N, 28.68.

5.2. Molecular modeling studies

The reference ligands **T_1AM**, **S18616**, RO5256390 and RO5263397 and the most promising **BIG** compounds were built *in silico*, parameterized (Gasteiger-Huckel method) and energy minimized within MOE using MMFF94 forcefield [55], taking into account all the possible tautomers.

Molecular docking studies were performed using the previously built *m*TAAR1 and *h*TAAR1 homology models, focusing on the binding site we carefully had evaluated around **T_1AM** [31,25]. Successively, flexible docking studies were applied using the Surflex docking module implemented in Sybyl-X1.0 [56].

Surflex-Dock uses an empirically derived scoring function based on the binding affinities of X-ray protein-ligand complexes. The Surflex-Dock scoring function is a weighted sum of non-linear functions involving van der Waals surface distances between the appropriate pairs of exposed protein and ligand atoms, including hydrophobic, polar, repulsive, entropic and solvation and crash terms represented in terms of a total score conferred to any calculated conformer.

Finally, the stability of the derived protein-ligand complexes was successfully assessed using a short ~1 ps run of molecular dynamics (MD) at constant temperature, followed by an all-atom energy minimization (LowModeMD implemented in MOE software). In this way, an exhaustive conformational analysis of the ligand-receptor binding site complex was explored, as we already explained about other case studies for a preliminary evaluation of the derived docking poses [57,58].

5.3. In silico evaluation of pharmacokinetic properties

The prediction of ADMET properties were performed using the Advanced Chemistry Development (ACD) Percepta platform (www.acdlabs.com).

Any ADMET descriptor was evaluated by Percepta based on training libraries implemented in the software, which include a consistent pool of molecules whose pharmacokinetic and toxicity profiles are experimentally known.

5.4. Biochemistry. Bioluminescence Resonance Energy Transfer (BRET) Measurement.

HEK-293 cells were transiently transfected with m/*h*TAAR1 or *m*TAAR5 and a cAMP BRET biosensor (EPAC) and then plated in a 96-well plate as described [59]. For time course experiments, the plate was read immediately after the addition of the agonist and for approximately 20 min. All the compounds were tested at the initial concentration of 10 μM.

Then, for active compounds, a dose response was performed in order to calculate the EC_{50} values. All the experiments were conducted in the presence of the phosphodiesterase inhibitor IBMX (Sigma) at the final concentration of 200 μM. Readings were collected using a Tecan Infinite instrument that allows the sequential integration of the signals detected in the 465−505 nm and 515−555 nm windows using filters with the appropriate band-pass and by using iControl software. The acceptor/donor ratio was calculated as previously described [60]. Curve was fitted using a nonlinear regression and one site specific binding with GraphPad Prism 5. Data are representative of 4−6 independent experiments and are expressed as means ± SEM.

Acknowledgments

This work was financially supported by the University of Genova. RRG was supported by the Russian Science Foundation (project N14-25-00065). The Authors would like to thank O. Gagliardo for performing elemental analyses.

Supplementary data

Docking poses of **T_1AM**, **BIG11** and **BIG13** (Fig. 1S), of **T_1AM** and **BIG12** (Fig. 2S), of **S18616** (Fig. 3S) and ^{1}H and ^{13}C NMR spectra of the newly synthesized compounds are reported.

References

[1] B. Borowsky, N. Adham, K.A. Jones, R. Raddatz, R. Artymyshyn, K.L. Ogozalek, M.M. Durkin, P.P. Lakhlani, J.A. Bonini, S. Pathirana, N. Boyle, X. Pu, E. Kouranova, H. Lichtblau, F.Y. Ochoa, T.A. Branchek, C. Gerald, Trace amines: identification of a family of mammalian G protein-coupled receptors, Proc. Natl. Acad. Sci. U. S. A. 98 (2001) 8966-8971.

[2] J.R. Bunzow, M.S. Sonders, S. Arttamangkul, L.M. Harrison, G. Zhang, D.I. Quigley, T. Darland, K.L. Suchland, S. Pasumamula, J.L. Kennedy, S.B. Olson, R.E. Magenis, S.G. Amara, D.K. Grandy, Amphetamine, 3,4-methylenedioxymethamphetamine, lysergic acid diethylamide, and metabolites of the catecholamine neurotransmitters are agonists of a rat trace amine receptor, Mol. Pharmacol. 60 (2001) 1181-1188.

[3] L. Lindemann, M.C. Hoener, A renaissance in trace amines inspired by a novel GPCR family, Trends Pharmacol. Sci. 26 (2005) 274-281.

[4] M.D. Berry, Mammalian central nervous system trace amines. Pharmacologic amphetamines, physiologic neuromodulators. J. Neurochem. 90 (2004) 257–271.

[5] H.A. Robertson, A.V. Juorio, Octopamine and some related noncatecholic amines in invertebrate nervous systems, Int. Rev. Neurobiol. 19 (1976) 173-224.

[6] T. Roeder, Octopamine in invertebrates. Prog. Neurobiol. 59 (1999) 533-561.

[7] Y. Pei, A. Asif-Malik, J.J. Canales, Trace Amines and the Trace Amine-Associated Receptor 1: Pharmacology, Neurochemistry, and Clinical Implications. Front. Neurosci. 10 (2016) 148.

[8] D. Leo, L. Mus, S. Espinoza, M.C. Hoener, T.D. Sotnikova, R.R. Gainetdinov, Taar1-mediated modulation of presynaptic dopaminergic neurotransmission: role of D2 dopamine autoreceptors, Neuropharmacology 81 (2014) 283-291.

[9] S. Espinoza, V. Ghisi, M. Emanuele, D. Leo, I. Sukhanov, T.D. Sotnikova, E. Chieregatti, R.R. Gainetdinov, Postsynaptic D2 dopamine receptor supersensitivity in the striatum of mice lacking TAAR1. Neuropharmacology. 93 (2015) 308-313.

[10] M.D. Berry, The potential of trace amines and their receptors for treating neurological and psychiatric diseases, Rev. Recent Clin. Trials. 2 (2007) 3-19.

[11] S.D. Liberles, L.B. Buck, A second class of chemosensory receptors in the olfactory epithelium, Nature 442 (2006) 645–650.

[12] A. Babusyte, M. Kotthoff, J. Fiedler, D. Krautwurst, Biogenic amines activate blood leukocytes via trace amine-associated receptors TAAR1 and TAAR2, J. Leukoc. Biol. 93 (2013) 387-394.

[13] M. Bly, Examination of the trace amine-associated receptor 2 (TAAR2), Schizophr. Res. 80 (2005) 367-368.

[14] I. Wallrabenstein, J. Kuklan, L. Weber, S. Zborala, M. Werner, J. Altmuller, C. Becker, A. Schmidt, H. Hatt, T. Hummel, G. Gisselmann, Human trace amine-associated receptor TAAR5 can be activated by trimethylamine, PloS One 8 (2013) e54950.

[15] J. Dinter, J. Mühlhaus, C.L. Wienchol, C.X. Yi, D. Nürnberg, S. Morin, A. Grüters, J. Köhrle, T. Schöneberg, M. Tschöp, H. Krude, G. Kleinau, H. Biebermann, Inverse agonistic action of 3-iodothyronamine at the human trace amine-associated receptor 5, PLoS One 10 (2015) e0117774.

[16] T.D. Sotnikova, M.G. Caron, R.R. Gainetdinov, Trace amine-associated receptors as emerging therapeutic targets, Mol. Pharmacol. 76 (2009) 229–235.

[17] D.T. Sotnikova, I.Z. Olesya, V. Ghisi, M.G. Caron, R.R. Gainetdinov, Trace amine associated receptor 1 and movement control, Parkinsonism Relat. Disord. 14 (2008) S99-S102.

[18] F.G. Revel, J.L. Moreau, B. Pouzet, R. Mory, A. Bradaia, D. Buchy, V. Metzler, S. Chaboz, K. Groebke Zbinden, G. Galley, R.D. Norcross, D. Tuerck, A. Bruns, S.R. Morairty, T.S. Kilduff, T.L. Wallace, C. Risterucci, J.G. Wettstein, M.C. Hoener, A new perspective for schizophrenia: TAAR1 agonists reveal antipsychotic- and antidepressant-like activity, improve cognition and control body weight, Mol. Psychiatry 18 (2013) 543-556.

[19] Y. Pei, J. Lee, D. Leo, R.R. Gainetdinov, M.C. Hoener, J.J. Canales, Activation of the trace amine-associated receptor 1 prevents relapse to cocaine seeking, Neuropsychopharmacology 39 (2014) 2299-2308.

[20] S. Espinoza, G. Lignani, L. Caffino, S. Maggi, I. Sukhanov, D. Leo, L. Mus, M. Emanuele, G. Ronzitti, A. Harmeier, L. Medrihan, T.D. Sotnikova, E. Chieregatti, M.C. Hoener, F. Benfenati, V. Tucci, F. Fumagalli, R.R. Gainetdinov, TAAR1 Modulates Cortical Glutamate NMDA Receptor Function, Neuropsychopharmacology 40 (2015) 2217-2227.

[21] S. Raab, H. Wang, S. Uhles, N. Cole, R. Alvarez-Sanchez, B. Künnecke, C. Ullmer, H. Matile, M. Bedoucha, R.D. Norcross, N. Ottaway-Parker, D. Perez-Tilve, K. Conde Knape, M.H. Tschöp, M.C. Hoener, S. Sewing, Incretin-like effects of small molecule trace amine-associated receptor 1 agonists, Mol. Metab. 5 (2015) 47-56.

[22] G. Galley, H. Stalder, A. Goergler, M.C. Hoener, R.D. Norcross, Optimisation of imidazole compounds as selective TAAR1 agonists: Discovery of RO5073012, Bioorg. Med. Chem. Letters 22 (2012) 5244–5248.

[23] A. Bradaia, G. Trube, H. Stalder, R.D. Norcross, L. Ozmen, J.G. Wettstein, A. Pinard, D. Buchy, M. Gassmann, M.C. Hoener, B. Bettler, The selective antagonist EPPTB reveals TAAR1-mediated regulatory mechanisms in dopaminergic neurons of the mesolimbic system, Proc. Natl. Acad. Sci. U. S. A. 106 (2009) 20081-20086.

[24] E. Cichero, S. Espinoza, S. Franchini, S. Guariento, L. Brasili, R.R. Gainetdinov, P. Fossa, Further insights into the pharmacology of the human trace amine-associated receptors: discovery of novel ligands for TAAR1 by a virtual screening approach, Chem. Biol. Drug Des. 84 (2014) 712-720.

[25] G. Chiellini, G. Nesi, M. Digiacomo, R. Malvasi, S. Espinoza, M. Sabatini, S. Frascarelli, A. Laurino, E. Cichero, M. Macchia, R.R. Gainetdinov, P. Fossa, L. Raimondi,

R. Zucchi, S. Rapposelli, Design, Synthesis, and Evaluation of Thyronamine Analogues as Novel Potent Mouse Trace Amine Associated Receptor 1 (mTAAR1) Agonists, J. Med. Chem. 58 (2015) 5096-5107.

[26] M. Cöster, H. Biebermann, T. Schöneberg, C. Stäubert, Evolutionary Conservation of 3-Iodothyronamine as an Agonist at the Trace Amine-Associated Receptor 1, Eur. Thyroid J. 4 (2015) 9-20.

[27] D.B. Wainscott, S.P. Little, T. Yin, Y. Tu, V.P. Rocco, J.X. He, D.L. Nelson, Pharmacologic characterization of the cloned human trace amine-associated receptor1 (TAAR1) and evidence for species differences with the rat TAAR1, J. Pharmacol. Exp. Ther. 320 (2007) 475-485.

[28] V. M. Lam, D. Rodríguez, T. Zhang, E. J. Koh, J. Carlsson, A. Salahpour, Discovery of trace amine-associated receptor 1 ligands by molecular docking screening against a homology model, Med. Chem. Commun. 6 (2015) 2216-2223.

[29] G. Galley, A. Beurier, G. Décoret, A. Goergler, R. Hutter, S. Mohr, A. Pähler, P. Schmid, D. Türck, R. Unger, K.G. Zbinden, M.C. Hoener, R.D. Norcross, Discovery and Characterization of 2-Aminooxazolines as Highly Potent, Selective, and Orally Active TAAR1 Agonists, ACS Med. Chem. Lett. 7 (2015) 192-197.

[30] L.A. Hu, T. Zhou, J. Ahn, S. Wang, J. Zhou, Y. Hu, Q. Liu, Human and mouse trace amine-associated receptor 1 have distinct pharmacology towards endogenous monoamines and imidazoline receptor ligands, Biochem. J. 424 (2009) 39-45.

[31] E. Cichero, S. Espinoza, R.R. Gainetdinov, L. Brasili, P. Fossa, Insights into the structure and pharmacology of the human trace amine-associated receptor 1 (hTAAR1): homology modelling and docking studies. Chem. Biol. Drug Des. 81 (2013) 509-516.

[32] E. Cichero, S. Espinoza, M. Tonelli, S. Franchini, A.S. Gerasimov, C. Sorbi, R.R. Gainetdinov, L. Brasili, P. Fossa, A homology modelling-driven study leading to the discovery of the first mouse trace amine-associated receptor 5 (TAAR5) antagonists Med. Chem. Commun. 7 (2016) 353-364.

[33] R.A. Glennon, M.K. Daoud, M. Dukat, M. Teitler, K. Herrick-Davis, A. Purohit, H. Syed, Arylguanidine and arylbiguanide binding at 5-HT3 serotonin receptors: a QSAR study, Bioorg. Med. Chem. 11 (2003) 4449-4454.

[34] A. Denys, T. Machlański, J. Bialek, S. Mrozicki, Relationships between chemical structure and antiviral activity of some biguanide derivatives, Zentralbl. Bakteriol. Orig. B 164 (1977) 85-89.

[35] S. Sheppard, Moroxydine: the story of a mislaid antiviral. Acta Derm. Venereol. Suppl. 183 (1994) 1-9.

[36] X.-B. Yu, X.-H. Chen, F. Ling, K. Hao, G.-X. Wang, B. Zhu, Moroxydine hydrochloride inhibits grass carp reovirus replication and suppresses apoptosis in Ctenopharyngodon idella kidney cells, Antiviral Res. 131 (2016) 156-165.

[37] A. Pinelli, R. Colombo, S. Trivulzio, F. Berti, O. Tofanetti, B.R. Caimi, Inhibitory effects of 2-guanidinebenzimidazole and 1-phenylbiguanide on gastric acid secretion in rats, Arzneim.-forsch 34 (1984) 890-894.

[38] A. Pinelli, S. Trivulzio, G. Pojaga, G. Rossoni, Effects of 2-guanidine-4-methylquinazoline on gastric acid secretion in rats, Pharmacol. Res. 34 (1996) 225-230.

[39] Z. Brzozowski, F. Saczewski, M. Gdaniec, Synthesis, structural characterization and antitumor activity of novel 2,4-diamino-1,3,5-triazine derivatives, Eur. J. Med. Chem. 35 (2000) 1053-1064.

[40] M. Pollak, Potential applications for biguanides in oncology, J. Clin. Invest. 123 (2013) 3693-3700.

[41] F.H.S. Curd, F.L. Rose, Synthetic antimalarials. Part IV. 2-Phenylguanidino-4-aminoalkylamino-6-methylpyrimidines, J. Chem. Soc. (1946) 362-365.

[42] B.R. Baker, B.-T. Ho, Analogs of tetrahydrofolic acid. XXIII. 1-(ω-phenylalkyl)-4,6-diamino-1,2-dihydro-s-triazines as inhibitors of dihydrofolic reductase, J. Heterocyclic Chem. 2 (1965) 72-79.

[43] E.J. Modest, P. Levine, Chemical and biological studies on 1,2-dihydro-s-triazines. III. Two-component synthesis, J. Org. Chem. 21 (1956) 14-20.

[44] S.L. Shapiro, V.A. Parrino, L. Freedman, Hypoglycemic Agents. III.[1-3] N^1-Alkyl- and Aralkylbiguanides. J. Am. Chem. Soc. 81 (1959) 3728-3736.

[45] E.J. Modest, Chemical and Biological Studies on 1,2-Dihydro-s-triazines. II. Three-Component Synthesis, J. Org. Chem. 21 (1956) 1-13.

[46] H. King, I.M. Tonkin, Antiplasmodial action and chemical constitution. Part VIII. Guanidines and diguanides, J. Chem. Soc. (1946) 1063-1069.

[47] S.W. Kim, H.W. Kim, S.H. Yoo, J.S. Lee, H.J. Heo, H.B. Lee, J.A. KOOK, Y.W. Lee, M.J. Kim, W. Cho, Guanidine compounds and use thereof, WO2015/160220 A1, 2015.

[48] V. L. Narayanan, Adamantyl-s-triazines, US 3471491, 1969.

[49] O. LeBel, T. Maris, H. Duval, J.D. Wuest, A practical guide to arylbiguanides-Synthesis and structural characterization[1], Can. J. Chem. 83 (2005) 615-625.

[50] P.V. Bharatam, D.S. Patel, P. Iqbal, Pharmacophoric features of biguanide derivatives: an electronic and structural analysis, J. Med. Chem. 48 (2005) 7615-7622.

[51] E.A. Reese, Y. Norimatsu, M.S. Grandy, K.L. Suchland, J.R. Bunzow, D.K. Grandy, Exploring the determinants of trace amine-associated receptor 1's functional selectivity for the stereoisomers of amphetamine and methamphetamine, J. Med. Chem. 57 (2014) 378-390.

[52] D.B. Wainscott, S.P. Little, T. Yin, Y. Tu, V.P. Rocco, J.X. He, D.L. Nelson, Pharmacologic characterization of the cloned human trace amine-associated receptor1 (TAAR1) and evidence for species differences with the rat TAAR1, J. Pharmacol. Exp. Ther. 320 (2007) 475-485.

[53] H. Waterbeemd, E. Gifford, ADMET in silico modelling: Towards prediction paradise? Nat. Rev. Drug Discov. 2 (2003) 192-204.

[54] T.A. Shapiro, D.E. Goldberg, Chemotherapy of Protozoal Infections: Malaria, in: L.L. Brunton, J.S. Lazo, K.L. Parker (Eds.), The Pharmacological Basis of Therapeutics, eleventh ed., McGraw-Hill, New York, 2006, pp 1021-1032

[55] MOE: Chemical Computing Group Inc. Montreal. H3A 2R7 Canada. http://www.chemcomp.com

[56] Sybyl-X 1.0 Tripos Inc 1699 South Hanley Road. St Louis. Missouri. 63144. USA 25

[57] P. Fossa, E. Cichero, In silico evaluation of human small heat shock protein HSP27: homology modeling, mutation analyses and docking studies, Bioorg. Med. Chem. 23 (2015) 3215-3520.

[58] S. Franchini, U.M. Battisti, A. Prandi, A. Tait, C. Borsari, E. Cichero, P. Fossa, A. Cilia, O. Prezzavento, S. Ronsisvalle, G. Aricò, C. Parenti, L. Brasili, Scouting new sigma receptor ligands: Synthesis, pharmacological evaluation and molecular modeling of 1,3-dioxolane-based structures and derivatives. Eur. J. Med. Chem. 112 (2016) 1-19.

[59] S. Espinoza, A. Salahpour, B. Masri, T.D. Sotnikova, M. Messa, L.S. Barak, M.G. Caron, R.R. Gainetdinov, Functional interaction between trace amine-associated receptor 1 and dopamine D2 receptor, Mol. Pharmacol. 80 (2011) 416-425.

[60] A. Salahpour, S. Espinoza, B. Masri, V. Lam, L.S. Barak, R.R. Gainetdinov, BRET biosensors to study GPCR biology, pharmacology, and signal transduction. Front. Endocrinol. 3 (2012) 105.

Supplementary Material - For Publication Online

Click here to download Supplementary Material - For Publication Online: Supplementary TAAR.docx